

Macromolecular Materials and Engineering / Volume 297, Issue 12 / p. 1167-1174

Full Paper | [Full Access](#)

Flexural-Torsional Photomechanical Responses in Azobenzene-Containing Crosslinked Polyimides

David H. Wang, Kyung Min Lee, Hilmar Koerner, Zhenning Yu, Richard A. Vaia, Timothy J. White ,
Loon-Seng Tan 

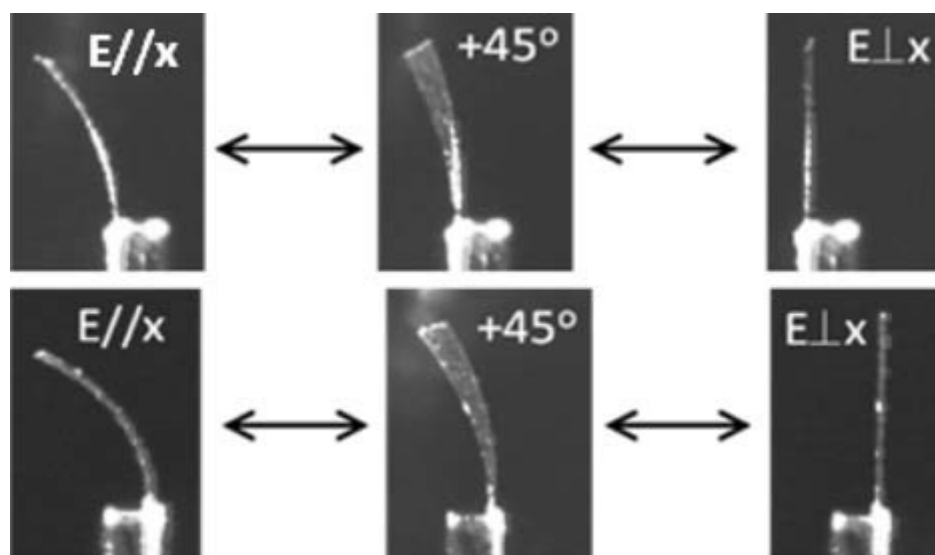
First published: 23 October 2012

<https://doi.org/10.1002/mame.201200240>

Citations: 19

Abstract

The influence of a variety of factors on the photomechanical output of azo-CP2-xx systems is studied, primarily focusing on a sample with a higher crosslink density (30 mol%) and two new, structurally related crosslinked polyimides with modified backbone flexibility/rigidity. This work elucidates the strong coupling between geometrical considerations (reciprocal aspect ratio of cantilever) and the visualized mechanical response (e.g., flexural-torsional response of a cantilever).



1. Introduction

Polyimides (PIs) represent an important class of heat-resistant polymers that have found use in a broad spectrum of applications, ranging from structural components to electronic and photonic devices because of their excellent combination of physical properties, thermal stability, and processability.^{1, 2} For example, a variety of PIs containing azobenzene in the backbone or side-chain have been investigated for photo-induced alignment in liquid crystal display (LCD) as well as nonlinear optical applications.³ From a historical perspective, it is noteworthy that the potential of linear azo-PIs in photomechanical applications was first indicated in 1970 by Agolini and Gay,⁴ in which they reported that a series of aromatic (semi-crystalline) PIs containing main-chain azobenzene-links was capable of undergoing reversible photo and thermal, axial contractile behaviors, albeit in small magnitudes. More recently, an azobenzene-containing poly(amic acid), a PI precursor, was crosslinked by a triamine in *N,N*-dimethylformamide (DMF) and the resulting sol-gels showed a two-fold increase in the storage modulus after irradiation with 405 nm light.⁵ Another closely related aromatic poly(amic acid) was claimed to be photomechanically active.⁶ Recently, we have reported on two series of azobenzene-containing aromatic PIs and investigated the influence of structural and morphological factors in the enhancement of photogenerated stress and the resulting photodirected bending behaviors in these PIs.^{7, 8} The first series (azo-CP2-xx) comprises amorphous, high glass-transition temperature (T_g : 220–246 °C) PIs crosslinked by a novel tris(azobenzeneamine) crosslinker (5–20 mol%). The second series comprises linear imide polymers and copolymers containing main-chain azobenzene units. Depending on the pyromellitimide (PMDI) content, their morphology can span from being amorphous to being semi-crystalline in addition to exhibiting a considerable increase in both T_g (>350 °C) and storage modulus (>6 GPa). The photogenerated tensile stress in these materials is as much as an order of magnitude larger than that previously observed in a glassy azo-LCN.⁹ Through systematic composition variation of the flexible (6FDA) and rigid (PMDA) dianhydrides together with 4,4'-diamino-azobenzene, we have shown that crystallinity decreases the magnitude of bending as well as the photogenerated tensile stress. The objective of this paper is to present our recent work examining the flexural-torsional photomechanical output of an azobenzene-containing crosslinked PI with higher crosslinker (and azobenzene) concentration. The ability to generate bend and twist (e.g., flexural-torsion) is strongly interrelated to sample geometry. As such, the photomechanical response of these new materials is contextualized with a cursory examination of the impact of reciprocal aspect ratio.

2. Experimental Section

2.1. Materials

1,3-Bis(3-aminophenoxy)benzene (APB, 99% min.), pyromellitic dianhydride (PMDA) and oxy-4,4'-di(phthalic anhydride) (ODPA) were purchased from Chriskev Company, Inc. 1,1,1,3,3,3-Hexafluoro-2,2-bis(4-phthalic anhydride)propane (6FDA) was purchased from Akron Polymer Systems. All three dianhydrides were sublimed before used. All other reagents and solvents were purchased from Aldrich and used as received, unless otherwise specified.

2.2. Tris(azobenzeneamine) Crosslinker (**6**)

The experimental details for the 4-step synthesis of the crosslinker **6** have been previously described in our report.[7](#)

2.3. Representative Procedure for the Synthesis of Azobenzene-Containing CP2 Polyimides (azo-CP2-30, **11d**)

APB (0.3216 g, 1.100 mmol) and DMAc (8 mL) were added to a 50-mL 3-necked flask equipped with a magnetic stirrer, nitrogen inlet and outlet, and stirred under dry nitrogen at room temperature for 30 min. 6FDA (0.8885, 2.000 mmol) was then introduced to the resulting solution. The light yellow solution was agitated at room temperature for 24 h to afford an anhydride-terminated poly(amic acid) solution (**9**). Then, the tris(azobenzene-amine) crosslinker (**6**; 0.5352 g, 0.600 mmol) was added to this solution. After **6** had completely dissolved in DMAc, the mixture poured into a glass Petri dish, followed by vacuum evaporation of DMAc at 50 °C, and heat-treated according to following schedule: 100 °C/2 h, 150 °C/2 h, 175 °C/1 h, 200 °C/1 h, 250 °C/1 h, and 300 °C/1 h to form PI films. The film thickness was approximately 20 μm. Attenuated total reflectance infrared (ATR-IR) spectroscopy (film): 3069 (C–H), 1785 (asym. imide C=O), 1721 (sym. imide C=O), 1586, 1438, 1363, 1297, 1236, 1190, 1099, 1013, 840, 719, 549 cm⁻¹. This procedure was followed to prepare other azo-CP2-xx.

2.4. Synthesis of azo-PMDI-20

APB (0.4093 g, 1.400 mmol) and DMAc (8 mL) were added to a 50 mL 3-necked flask equipped with a magnetic stirrer, nitrogen inlet and outlet, and stirred under dry nitrogen at room temperature for 30 min. PMDA (0.4362 g, 2.000 mmol), was then introduced to the resulting solution. The yellow solution was agitated at room temperature for 24 h to afford an anhydride-terminated poly(amic acid) solution (**10**). Then, the tris(azobenzene-amine) crosslinker (**6**, 0.3568 g, 0.400 mmol) was added to this solution. After **6** had completely dissolved in DMAc, the mixture poured into a glass Petri dish, followed by vacuum evaporation of DMAc at 50 °C, and heat-treated according to following schedule: 100 °C/2 h, 150 °C/2 h, 175 °C/1 h, 200 °C/2 h, 250 °C/1 h, and 300 °C/1 h to form PI films. The film thickness was approximately 20 μm. ATR-IR (film): 3068 (C–H), 1777 (asym. imide C=O), 1714 (sym. imide C=O), 1584, 1488, 1478, 1451, 1361, 1222, 1098, 1012, 978, 830, 775, 721, 680, 566 cm⁻¹.

2.5. Synthesis of azo-OPDI-20

Azo-OPDI-20 was synthesized from OPDA (0.6204 g, 2.000 mmol), APB (0.4093 g, 1.400 mmol), tris(azobenzeneamine) crosslinker (**6**, 0.3568 g, 0.400 mmol), and DMAc (8 mL) using the same procedure used for azo-PMDA-20 to afford 20 μm thickness films. ATR-IR (film): 3066 (C—H), 1778 (ms, asym. imide C=O), 1715 (vs, sym. imide C=O), 1584, 1474, 1438, 1359, 1232, 1180, 1139, 1095, 1012, 981, 833, 772, 741, 683, 624, 551 cm^{-1} .

2.6. Instrumentation

Dynamic mechanical analysis (DMA) of the azo-PI films were conducted in a nitrogen atmosphere with a heating rate of 4 $^{\circ}\text{C} \cdot \text{min}^{-1}$ on TA Instruments DMA Q800. Infrared (IR) spectra were recorded on a Nicolet Nexus 470 Fourier-transform spectrophotometer. Thermogravimetric analysis (TGA) was conducted in nitrogen (N_2) and air atmospheres at a heating rate of 10 $^{\circ}\text{C} \cdot \text{min}^{-1}$ using a TA Hi-Res TGA 2950 thermogravimetric analyzer.

2.7. Photomechanical Bending of Polyimide Network Cantilevers

Photodriven bending was directed with linearly polarized 442 nm line of a 130 mW helium-cadmium (HeCd, Kimmon) laser. The HeCd laser beam was expanded and collimated with a spherical lens, uniformly exposing the entirety of the cantilever with an intensity of 100 $\text{mW} \cdot \text{cm}^{-2}$.¹⁰ The orientation of the linear polarization to the sample was controlled with a Fresnel rhomb (Newport). The optical setup has been illustrated and described in detail elsewhere.¹⁰ The photomechanical bending of azo-PI network cantilevers was monitored with a charge coupled device. The bending angle was analyzed with a program that determined the tip displacement angle between the mounting point of the cantilever and the outside edge of the tip of cantilever.

3. Results and Discussion

It is known that the crosslinked moieties or domains, either chemical or physical, play a pivotal role in the thermally induced shape-memory¹¹ and photomechanical polymers such as liquid-crystalline networks.¹² In both types of stimuli-responsive polymers, the primary function of a crosslink is to serve as the net points that would collectively remember to return to their original positions whenever the local strains are released. In addition, the ability of the photomechanical polymeric systems to transduce light into mechanical work is hinged on the ability of dichromic chromophores, in this case, azobenzene units to quantitatively isomerize and induce configurational/conformational changes, which are manifested as local strains on the chain (or network) architecture that are summed and transferred into a macroscopic response. In this work, such transduction outcome is potentially enhanced at the molecular level by incorporating all three azobenzene chromophores in a single crosslinker unit.

3.1. Azobenzeneamine Crosslinker

The synthesis of such a crosslinker (**6** in Scheme 1), which contains three azobenzene moieties, i.e., a tris(azobenzeneamine), and with a stretched-out tripod geometry was performed in four steps. Briefly, 1,1,1-tris(4-hydroxyphenyl)ethane (**1**) was treated with 1-fluoro-4-nitrobenzene in the presence of potassium carbonate to yield 1,1,1-tris[4-(4-nitrophenoxy)phenyl]ethane (**2**), which was then reduced to 1,1,1-tris[4-(4-aminophenoxy)phenyl]ethane (**3**) by catalytic hydrogenation. The condensation reaction of **3** and 4-nitrosoacetanilide¹³ (**4**) in acetic acid yielded **5**, a precursor containing three azobenzene units. The tris(azobenzeneamine) crosslinker (**6**) was generated after the deprotection of **5** via an alkaline deacetylation.



Scheme 1

[Open in figure viewer](#) | [↓ PowerPoint](#)

A four-step synthesis of azobenzene-containing crosslinker **6**.

3.2. Azobenzene CP2 and Related Polyimide Networks

The PI examined here is based on a well-known low-color, space-grade PI (CP2) with a glass-transition temperature in excess of 200 °C and derived from 2,2-bis(phthalic anhydride)-1,1,1,3,3,3-hexafluoroisopropane (6FDA) and APB.^{14, 15} Although CP2 when prepared via chemically imidization in solution is known to be soluble in common organic solvents such as amide- (DMF, DMAc, NMP) and ether-type (THF) solvents, we found it to be more convenient to follow the protocol depicted in Scheme 2 in the preparation of the crosslinked PI films, from which the requisite cantilevers were cut out. The key point in this protocol is that adding the crosslinker at the “anhydride-endcapped poly(amic acid)” stage rather than to the solution containing fully imidized, anhydride-endcapped CP2, whose molecular weight is variable via controlling reaction stoichiometry. Thus, apart from having the flexibility in adding the amount of crosslinker in each sample, the rate of crosslinking could be more easily controlled, premature gelation was avoided, and uniform distribution of crosslinks was obtained satisfactorily in the cast films. For the preparation of azo-CP2-xx samples (where xx = mol% crosslinker, i.e., 5, 10, 20, or 30), the respective amounts of 6FDA, APB, and crosslinker **6** are indicated in Table 1. To further elucidate the structural influence of diimide unit, we have also prepared two new and related PI networks, one using a structurally more rigid anhydride, namely, PMDA while the other being more flexible than 6FDA. Their syntheses follow the same protocol as depicted in Scheme 2.



Scheme 2

[Open in figure viewer](#) | [PowerPoint](#)

Synthesis of azobenzene-containing crosslinked PI networks: azo-CP2-xx (**11a-d**), azo-PMDI-20 (**11e**), and azo-OPDI-20 (**11f**).

Table 1. Compositions and properties of crosslinked PI films.

Sample	6FDA [mol%]	APB [mol%]	Compd 6 [mol%]	$T_g^a)$ [°C]	$E^b)$ [GPa]	$c)$ [Da]	$\alpha_{442}^d)$ [cm ⁻¹]
CP2	100	100	0	219	1.9 ± 0.1	-	-
azo-CP2-03 ^{e)}	100	95.5	3	-	-	15 827 ^{f)}	-
azo-CP2-05 (11a) ^{g)}	100	92.5	5	220	1.6 ± 0.2	9592 ^{f)}	379
azo-CP2-10 (11b) ^{g)}	100	85	10	226	1.8 ± 0.2	4916 ^{f)}	470
azo-CP2-20 (11c) ^{g)}	100	70	20	246	2.4 ± 0.3	2578 ^{f)}	563
azo-CP2-30 (11d) ^{g)}	100	55	30	284	2.9 ± 0.3	1799 ^{f)}	650
azo-CP2-40 ^{e)}	100	40	40	-	-	1409 ^{f)}	-

a) T_g measured from the peak of $\tan \delta$ (DMA) as an average value taken from four measurements;

b) Modulus determined in tension at 25 °C as average from five specimens per sample;

c) denotes the average molecular weight of the linear segment between two crosslinked sites, calculated from $\bar{M}_n = 350.27 \times X_n \pm 295.32 \times 2$, where 350.27 is one-half the formula weight of a CP2 repeat unit; the number-average degree of polymerization $X_n = (1+r)/(1-r)$; the stoichiometric imbalance factor (r) is the molar ratio of diamine to dianhydride; 295.32 is one-third value of the formula weight of crosslinker segment (from methyl-end to imide-nitrogen) in CP2 network;

d) Measured absorption coefficient for the materials at 442 nm;

e) Extrapolated crosslinked PI compositions to provide an arbitrary range of degrees of polymerization (n), which is indicated by l, m, n in the generic structure for azo-CP2-xx, see Scheme 2) for linear CP2 segments;

- f) Since MW for a CP2 repeat unit is ≈ 700 Da, the calculated values are (from top to bottom): 23, 14, 7, 4, 3, and 2;
- g) The measured thickness of the azo-CP2 films are 18 μm (azo-CP2-05), 21 μm (azo-CP2-10), 21 μm (azo-CP2-20), and 20 μm (azo-CP2-30). The cantilever was uniform in thickness with variation less than 0.5 μm .

As would be expected, the crosslinking density of these materials increase as the crosslinker concentration increases, in agreement with the calculated average molecular weights between crosslinked sites (M_c),¹⁶ which follows an opposite trend (see Table 1). The glass transition temperature (T_g) of neat PI (CP2) is 219 °C by DMA. Comparatively, the T_g values (220–284 °C) of the azobenzene-containing PI networks, i.e., azo-CP2-xx, increase with the concentration of tris(azobenzene-amine) crosslinker, especially with concentrations >5 mol%.

Storage modulus (E'), loss modulus (E''), and loss tangent ($\tan \delta$) were characterized with DMA, and the results are summarized in Table 1. The tensile moduli (E) of the azo-CP2 films initially decrease with the presence of crosslinker concentration (0–5 mol%) as compared to that of unmodified CP2 before subsequently increasing by ≈ 0.2 – 0.3 GPa per 5 mol% of crosslinker added. We speculate that at the crosslinker concentration of ≤ 5 mol%, the tripod geometry of the crosslinker may be disrupting the chain-packing regularity of the CP2 PI, resulting in softening of the azo-CP2 networks. However, in the azo-CP2 systems increasing crosslink density and corresponding decrease in M_c between net points starts to dominate and causes the increase in modulus with each addition of 5 or 10 mol% crosslinker.

3.3. Photomechanical Characterization of azo-CP2-xx Cantilevers

3.3.1. Polarization Dependence

It is well-established that a linearly polarized blue-green (440–510 nm) light induces what has been referred to as *trans-cis-trans* reorientation (also known as an Weigert effect).¹⁷ This phenomenon has been extensively employed in glassy azo-polymers to form both conventional volume gratings as well as surface relief gratings.^{11, 18, 19} Fundamental to this mechanism is the simultaneous and repeated *trans-cis* and *cis-trans* isomerization cycles of azobenzene induced by light in this wavelength regime. The repeated *trans-cis* and *cis-trans* isomerizations of azobenzene, due to the dichroic absorption of azobenzene (in addition to the rotational freedom of the azo bond when photo-excited) results in a statistical buildup of *trans* azobenzene rotated orthogonal to the incident linear polarization of the light source.

In our previous work, the photomechanical response of azo-CP2-xx cantilevers (where xx = 5, 10, and 20 mol% crosslinker) has been characterized in terms of the magnitude of bending angle and direction versus polarization angle on exposure to a linearly polarized blue laser of 442 nm in wavelength with an intensity of $100 \text{ mW} \cdot \text{cm}^{-2}$.^{7, 10} For example, in the case of azo-CP2-20, the cantilever bends around 20° when exposed to the light polarized parallel to the long axis

($E \parallel x, 0^\circ$) of the cantilever. As polarization angle is shifted from 0 to 15° , the magnitude of bending decreases and no bending is observed when the polarization of the laser is 45° to the long axis of the cantilever. At polarization angles greater than 45° , bending occurs in the reverse direction with greatest magnitude when the azo-CP2-20 cantilever is exposed to light polarized orthogonal to the long axis ($E \perp x, 90^\circ$) of the cantilever. Importantly, both the forward and reverse bending directions are uniform and symmetrical.

Thermal imaging experiments¹⁰ of the azo-CP2-20 sample under irradiation to the conditions reported here exhibit a maximum temperature rise of $\approx 2\text{--}3^\circ\text{C}$. Therefore, it is reasonable to assume here that the contributions to the observed mechanical motions due to thermal expansion and related temperature gradients in the cantilevers are not significant.

Due to the large absorption coefficient of azo-CP2-xx at 442 nm (see Table 1), light is absorbed non-uniformly across the thickness of the film. When light is polarized parallel to the long axis (defined here as x -direction) of the cantilever, the reorientation of azobenzene results in a contraction along this long axis, which yields bending toward the laser source. Conversely, when light is polarized orthogonal to the long axis of the cantilever, the reorientation of azobenzene causes an expansion in x -direction, which yields bending motion away from the laser source. The fact that bending is not observed to light polarized 45° to the long axis confirms that (a) the mechanism is not photo-thermal in nature, and (b) it is the expected result of a reorientation mechanism (i.e., no net change in reorientation).

3.3.2. Higher Crosslink Density

Given nearly the same geometrical parameters in the crosslinked PI samples (see Figure 1), the photomechanical behaviors of the cantilevers alter fairly linearly with respect to the crosslinker content between 5 and 20 mol%. However, we found that at higher crosslinker concentration (≤ 30 mol%), the photomechanical behavior of the azo-CP2-30 sample has apparently diverged from this trend as observed in samples containing ≤ 20 mol% crosslinker. Interestingly, azo-CP2-30 shows higher absolute bending angles, i.e., ca. 70° ($+65/-5^\circ$) than those of the azo-CP2 samples containing ≤ 20 mol% crosslinker, even though azo-CP2-30 exhibits higher modulus and glass transition temperature than samples with ≤ 20 mol% crosslinker (Table 1). Furthermore, the azo-CP2-30 cantilever exhibits an asymmetrical photo-bending behavior, implicating that as the crosslinking density reaches a certain critical value and the linear segments are correspondingly shorter, these mutually related structural features are becoming the controlling factors in the photomechanical output.



Figure 1

Bending angle of cantilevers composed from azo-CP2-xx as a function of azobenzene-triamine content after 1 h of irradiation from $100 \text{ mW} \cdot \text{cm}^{-2}$ of 442 nm light.

[Open in figure viewer](#) | [PowerPoint](#)

3.3.3. Cantilever Geometry

The cantilever geometry (e.g., aspect ratio) is a potentially strong influence in photomechanical effects generated with blue-green light. Recent examinations in highly aligned monodomain azo-LCN materials have shown so-called flexural-torsional responses.²⁰ Flexural-torsional responses are manifestation of non-uniform shear through the thickness which generates twisting. It is our expectation that the degree of twist is highly interrelated to the sample geometry. As such, we systematically varied the reciprocal aspect ratio (constant thickness, constant length, changing width) of cantilevers composed from azo-CP2-30 amorphous and isotropic PI materials by simply orientating the alignment of the linear polarization of the light source, Cantilevers composed from azo-CP2-30 with the same thickness (20 μm) and length (6 mm), various ranges of reciprocal aspect ratios from 0.0167 to 0.5 are examined for bending and twisting behaviors, and the results are summarized graphically in Figure 2. Azo-CP2-30 with small reciprocal aspect ratio (0.0167, i.e., 0.1 mm width) shows polarization-dependent bidirectional bending ($+29/-27^\circ$). However, with increasing reciprocal aspect ratio, it is apparent that both the asymmetrical bending and unidirectional bending are occurring. Interestingly, the azo-CP2-30 cantilevers with reciprocal aspect ratios of 0.25 (1.5 mm width) and 0.5 (3 mm width) exhibit planar bending upon irradiation with light polarized parallel ($E \parallel x$) or orthogonal ($E \perp x$) to the long axis of the cantilever. However, from the images in Figure 2 it is clear that when the linear polarization of the 442 nm laser is oriented $+45^\circ$ to the long axis of the cantilever, these samples show large twisting behavior.



Figure 2

[Open in figure viewer](#) | [PowerPoint](#)

Flexural-torsional photomechanical response of cantilevers composed from azo-CP2-30 (20 μm thickness) as a function of reciprocal aspect ratio. All cantilevers were 6 mm in length while the width of the cantilevers was reduced [photos on the left, from top to bottom (width): 3, 1.5, 1, 0.1 mm].

Apparently, the response of azo-CP2-30 cantilever to the light polarization follows a pattern different from that exhibited by other azo-CP2-xx under the same irradiation conditions. As shown in Figure 3, in addition to the observation that the angle of bending almost reaches 75° upon exposure to parallel-polarized blue-green light, there are three distinctly different photomechanical outcomes, namely (i) uni-directional bending (toward light source) occurs

regardless of polarization direction; (ii) mechanical motion is changed to a combined motion of bending and twisting; (iii) twisting direction, i.e., left-handed or right-handed essentially corresponds to the polarization direction. Thus, light polarization directions control bending and twisting directions of the azo-CP2-30 cantilever. These observations demonstrate that the cantilever geometry plays an important role in influencing and/or amplifying these divergent photomechanical behaviors. The photomechanical output, visualized here as bending of a cantilever, is as such strongly dependent on geometry. To further elucidate the ability to control the extent of twisting within an azo-CP2-30 cantilever we examined the photomechanical response at a broader range of intermediate polarization orientations: ± 23 , 45 , and 68° . Evident in the images in Figure 3, the directionality of the polarization (+ or -) dictates the directionality of the twist. Secondly, the magnitude of the flexural-torsional response is nuanced. At $\pm 23^\circ$ the cantilevers strongly bend with some twist, while at ± 45 and 68° the cantilevers increasingly twist at the expense of bend.



Figure 3

[Open in figure viewer](#) | [↓ PowerPoint](#)

Flexural-torsional response of a cantilever composed of azo-CP2-30 cantilever ($16\ \mu\text{m}$ thickness) at reciprocal aspect ratio of 0.17 to intermediate polarization alignments between parallel and orthogonal to the long axis of the cantilever. The sign of the polarization is shown to dictate the directionality of the twisting.

For completeness, we also examined the contribution of thickness to the extent of the photomechanical response, once again visualized by examining the extent of deflection of a cantilever composed of azo-CP2-30. As expected, increasing thickness reduces the magnitude of the bend. In the geometry examined here, the reciprocal aspect ratio was approximately 0.25 (Figure 4).



Figure 4

[Open in figure viewer](#) | [↓ PowerPoint](#)

The relationship between cantilever thickness and the magnitude of the bend of a cantilever composed from azo-CP2-30 of a reciprocal aspect ratio of 0.17 is examined. Increasing thickness reduces the magnitude of the bending angle.

3.3.4. Flexibility/Rigidity in Linear Segments

From the standpoint of macromolecular architecture, it appears that there is some direct correlation of photomechanical response and the T_g as well as the modulus of azo-CP2-xx. Thus, to further probe this correlation via molecular engineering and using azo-CP2-20 as the reference to represent the subset of azo-CP2-xx with crosslinker concentration of ≤ 20 mol%, we have synthesized two new crosslinked PIs based on crosslinker 6 and APB: (i) azo-PMDI-20, which was synthesized using a much more rigid dianhydride, namely, PMDA, and (ii) azo-OPDI-20, which was synthesized using a more flexible dianhydride namely, OPDA. As confirmed by their T_g and modulus values, azo-PMDI-20 ($T_g = 282$ °C, $E = 3.7 \pm 0.2$ GPa) is comprised of much stiffer linear-chain segments than azo-CP2-20 ($T_g = 246$ °C, $E = 2.4 \pm 0.2$ GPa) and the linear-chain segments of azo-OPDI-20 ($T_g = 239$ °C, $E = 2.2 \pm 0.2$ GPa) are relatively more flexible. In comparing the photomechanical outputs of these PI cantilevers with same dimensions (20 μm thick, $L = 6$ mm $W = 1$ mm), we observe that the "stiffer" azo-PMDI-20 cantilever ($E \parallel x$, $+17^\circ$; $E \perp x$, -15° ; absolute bending angle = 32°) responds more or less similar to the response by azo-CP2-20 ($E \parallel x$, $+19^\circ$; $E \perp x$, -17° ; absolute bending angle = 36°), and the asymmetrical photobending behavior of the more flexible azo-OPDI-20 ($E \parallel x$, $+32^\circ$; $E \perp x$, -11° ; absolute bending angle = 43°) under polarized blue-green irradiation. Based on the absolute angle values, we obtain the following increasing order: azo-PMDI-20 < azo-CP2-20 < azo-OPDI, which is in parallel to the expected trend in increasing molecular flexibility. In addition, azo-OPDI-20 exhibits asymmetric bending while azo-CP2-20 and azo-PMDI-20 show symmetrical bending (see Figure 5).



Figure 5

[Open in figure viewer](#) | [PowerPoint](#)

Effect of diimide structure in the photo-bending of crosslinked PIs; see Scheme 2 for the chemical structures for the diimides, OPDI and PMDI.

4. Conclusion

In our amorphous and high T_g , crosslinked PI system (azo-CP2-xx), the polarization-controlled forward/backward, symmetrical/asymmetric bending motions are shown to be strongly dependent on azobenzene/crosslinker concentration as well as thickness and reciprocal aspect ratio (width/length) of the cantilevers. The cantilever geometry can affect the symmetry in bending motion and lead to twisting motion.²⁰ Under the observed geometry space, the competing forces are discernable only in the azo-CP2-30 cantilevers.²¹ Therefore, we tentatively attribute this change in motional symmetry to the competition between the photo-generated bending forces in length-wise and width-wise directions. In addition to the effects of crosslink density/azobenzene concentration on the photomechanical divergence, the polymer chain flexibility/rigidity was modified, which affects the photomechanical response to a larger

extent for the structurally more flexible diimide structure (e.g., OPDI), as compared to the more rigid and planar PMDI structure. This modification results in larger absolute bending angles and an askew bending symmetry, thus confirming the possible role of molecular engineering in tailoring the photomechanical response in these crosslinked PIs.

Acknowledgements

We thank Dr. Matthew Smith (AFRL/RX, National Research Council Fellowship Program) for helpful discussion on polymer photomechanics, and Marlene Houtz (University of Dayton Research Institute) for DMA data. Funding support was provided by AFRL/AFOSR and AFRL/RX Directorates.

References



1

[Google Scholar](#)

a) D. Wilson, H. D. Stenzenberger, P. M. Hergenrother, *Polyimides*, Chapman and Hall, New York 1990, pp. 1– 78;

[Crossref](#) | [Google Scholar](#)

b) P. M. Hergenrother, in: *Polyimides and Other High-Temperature Polymers*, Eds. M. J. M. Abadie, B. Sillion), Elsevier, New York 1991, pp. 1– 18.

[Web of Science®](#) | [Google Scholar](#)

2 C. E. Sroog, *Prog. Polym. Sci.* 1991, **16**, 561.

[Crossref](#) | [CAS](#) | [Web of Science®](#) | [Google Scholar](#)

3

[Google Scholar](#)

a) K. Usami, K. Sakamoto, N. Tamura, A. Sugimura, *Thin Solid Films*, 2009, **518**, 729;

[Crossref](#) | [CAS](#) | [Web of Science®](#) | [Google Scholar](#)

b) B. Park, Y. Jung, H.-H. Choi, H.-K. Hwang, Y. Kim, S. Lee, S.-H. Jang, M.-A. Kakimoto, H. Takezoe, *Jpn. J. Appl. Phys. Part 1*, 1998, **37**, 5663;

[Crossref](#) | [CAS](#) | [Web of Science®](#) | [Google Scholar](#)

c) V. G. Chigrinov, V. M. Kozenkov, H. S. Kwok, *Photoalignment of Liquid Crystalline Materials: Physics and Applications*, Wiley, Chichester 2008;

[Wiley Online Library](#) | [Google Scholar](#)

d) Y. Koshiba, M. Yamamoto, K. Kinashi, M. Misaki, K. Ishida, Y. Oguchi, Y. Ueda, *Thin Solid Films*, 2009, **518**, 805;

[Crossref](#) | [CAS](#) | [Web of Science®](#) | [Google Scholar](#)

e) J. A. Delaire, K. Nakatani, *Chem. Rev.* 2000, **100**, 1817.

[Crossref](#) | [CAS](#) | [PubMed](#) | [Web of Science®](#) | [Google Scholar](#)

4

[Google Scholar](#)

a) F. Agolini, F. P. Gay, *Macromolecules* 1970, **3**, 349;

[Crossref](#) | [CAS](#) | [Web of Science®](#) | [Google Scholar](#)

b) see also G. S. Kumar, D. C. Neckers, *Chem. Rev.* 1989, **89**, 1915.

[Crossref](#) | [CAS](#) | [Web of Science®](#) | [Google Scholar](#)

5 N. Hosono, H. Furukawa, Y. Masubuchi, T. Watanabe, K. Horie, *Colloids Surf., B* 2007, **56**, 285.

[Crossref](#) | [CAS](#) | [PubMed](#) | [Web of Science®](#) | [Google Scholar](#)

6 C. Zhang, X. Zhao, D. Chao, X. Lu, C. Chen, C. Wang, W. Zhang, *J. Appl. Polym. Sci.* 2009, **113**, 1330.

[Wiley Online Library](#) | [CAS](#) | [Web of Science®](#) | [Google Scholar](#)

7 D. H. Wang, K. M. Lee, Z. Yu, H. Koerner, R. A. Vaia, T. J. White, L.-S. Tan, *Macromolecules* 2011, **44**, 3840.

[Crossref](#) | [CAS](#) | [Web of Science®](#) | [Google Scholar](#)

8 K. M. Lee, D. H. Wang, H. Koerner, R. A. Vaia, L.-S. Tan, T. J. White, *Angew. Chem., Int. Ed.* 2012, **51**, 4117.

[Wiley Online Library](#) | [CAS](#) | [PubMed](#) | [Web of Science®](#) | [Google Scholar](#)

9 L. Cheng, Y. Torres, K. M. Lee, A. J. McClung, J. Baur, T. J. White, W. S. Oates, *J. Appl. Phys.* 2012, **112**, 013513.

[Crossref](#) | [CAS](#) | [Web of Science®](#) | [Google Scholar](#)

10 K. M. Lee, N. V. Tabiryan, T. J. Bunning, T. J. White, *J. Mater. Chem.* 2012, **22**, 691. In this work, we measured the surface temperature of the cantilever composed of polydomain azo-LCN (20% azo-content) with the aid of an IR camera, and observed a 3.5 °C increase for 100 mW · cm⁻² intensity.

[Crossref](#) | [CAS](#) | [Web of Science®](#) | [Google Scholar](#)

11 J. Leng, X. Lan, Y. Liu, S. Du, *Prog. Mater. Sci.* 2011, **56**, 1077, and references therein.

[Crossref](#) | [CAS](#) | [Web of Science®](#) | [Google Scholar](#)

12

[Google Scholar](#)

a) J-i. Mamiya, Y. Yu, T. Ikeda, " Photomechanical Effects of Crosslinked Liquid-crystalline Polymers" in: *Crosslinked Liquid Crystalline Systems*, (Eds: D. J. Broer, G. P. Crawford, S. Zumer), CRC Press, Boca Raton 2011, pp. 183– 204;

[Crossref](#) | [Google Scholar](#)

b) *Smart Light-Responsive Materials: Azobenzene-Containing Polymers and Liquid Crystals*, (Eds: Y. Zhao, T. Ikeda), Wiley, Hoboken, NJ 2009;

[Wiley Online Library](#) | [Google Scholar](#)

c) K. G. Yager, C. J. Barrett, " Azobenzene Polymers as Photomechanical and Multifunctional Smart Materials", in: *Intelligent Materials*, (Eds: M. Shahinpoor, H-J. Schneider), Royal Society of Chemistry, Cambridge 2008, pp. 424– 446;

[Google Scholar](#)

d) C. J. Barrett, J-i. Mamiya, K. G. Yager, T. Ikeda, *Soft Matter* 2007, **3**, 1249;

[Crossref](#) | [CAS](#) | [PubMed](#) | [Web of Science®](#) | [Google Scholar](#)

e) Y. Yu, T. Maeda, J-i. Mamiya, T. Ikeda, *Angew. Chem., Int. Ed.* 2007, **46**, 881.

[Wiley Online Library](#) | [CAS](#) | [PubMed](#) | [Web of Science®](#) | [Google Scholar](#)

13 J. C. Cain, *J. Chem. Soc., Trans.* 1908, **93**, 681.

[Crossref](#) | [CAS](#) | [Google Scholar](#)

14

[Google Scholar](#)

a) CP2 is shortened from the original acronym, LaRC-CP2, which originated from a NASA research program on colorless polyimides (CP) for space coating applications, where optical transparency was critical: A. K. St Clair, T. L. St Clair, K. I. Shevket, *Polym. Mater. Sci. Eng.* 1984, **51**, 62;

[CAS](#) | [Google Scholar](#)

b) G. A. Miner, D. M. Stoakley, A. K. St Clair, P. A. Gierow, K. Bates, *Polym. Mater. Sci. Eng.* 1997, **76**, 381.

[CAS](#) | [Google Scholar](#)

15 ManTech SRS Technologies, LaRC-CP1 and LaRC-CP2 polyimide film properties 2004,

<http://www.mantechmaterials.com>

[Google Scholar](#)

16 For the theoretical calculation of the average molecular weights between crosslinked sites (M_c), see footnote (d) to Table 1 and: G. Odian, *Principles of Polymerization*, 4th edition, John Wiley Sons, Inc., Hoboken 2004, p. 75.

[Wiley Online Library](#) | [Google Scholar](#)

17 N. K. Viswanathan, D. U. Kim, S. Bian, J. Williams, W. Liu, L. Li, L. Samuelson, J. Kumar, S. K. Tripathy, *J. Mater. Chem.* 1999, **9**, 1941.

[Crossref](#) | [CAS](#) | [Web of Science®](#) | [Google Scholar](#)

18

[Google Scholar](#)

a) C. Cojocariu, P. Rochon, *Pure Appl. Chem.* 2004, **76**, 1479;

[Crossref](#) | [CAS](#) | [Web of Science®](#) | [Google Scholar](#)

b) A. Natansohn, P. Rochon, *Chem. Rev.* 2002, **102**, 4139.

[Crossref](#) | [CAS](#) | [PubMed](#) | [Web of Science®](#) | [Google Scholar](#)

19

[Google Scholar](#)

a) M. Irie, *Bull. Chem. Soc. Jpn.* 2008, **81**, 917;

[Crossref](#) | [CAS](#) | [Web of Science®](#) | [Google Scholar](#)

b) O. Pieroni, F. Ciardelli, *Trends Polym. Sci.* 1995, **3**, 282;

[CAS](#) | [Web of Science®](#) | [Google Scholar](#)

c) M. Irie, T. Ikeda, "Photoresponsive Polymers", in: *Functional Monomers and Polymers*, 2nd edition (Eds: K. Takemoto, R. M. Ottenbrite, M. Kamachi), Marcel Dekker, New York 1997, pp. 65– 116.

[Google Scholar](#)

20 K. M. Lee, M. L. Smith, H. Koerner, N. Tabiryan, R. A. Vaia, T. J. Bunning, T. J. White, *Adv. Funct. Mater.* 2011, **21**, 2913.

[Wiley Online Library](#) | [CAS](#) | [Web of Science®](#) | [Google Scholar](#)

21 M. L. Smith, H. Koerner, K. M. Lee, T. J. White, R. A. Vaia, Unpublished.

[Google Scholar](#)

Citing Literature



[Download PDF](#)

About Wiley Online Library

[Privacy Policy](#)

[Terms of Use](#)

[Cookies](#)

[Accessibility](#)

[Help & Support](#)

[Contact Us](#)

[Training and Support](#)

[DMCA & Reporting Piracy](#)

[Opportunities](#)

[Subscription Agents](#)

[Advertisers & Corporate Partners](#)

[Connect with Wiley](#)

[The Wiley Network](#)

[Wiley Press Room](#)

Copyright © 1999-2021 John Wiley & Sons, Inc. All rights reserved